

VĚDECKÉ SPISY VYSOKÉHO UČENÍ TECHNICKÉHO V BRNĚ

*Edice Habilitační a inaugurační spisy, sv. 512*

*ISSN 1213-418X*

**Roman Gröger**

**MULTISCALE MODELING  
OF PLASTICITY OF BCC METALS**

VYSOKÉ UČENÍ TECHNICKÉ V BRNĚ

Fakulta strojního inženýrství

Akademie věd České republiky

Ústav fyziky materiálů

&

Středoevropský technologický institut (CEITEC)

**Ing. Roman Gröger, Ph.D. et Ph.D.**

**MULTISCALE MODELING OF PLASTICITY  
OF BCC METALS**

VÍCEÚROVŇOVÉ MODELOVÁNÍ PLASTICITY BCC KOVŮ

ZKRÁCENÁ VERZE HABILITAČNÍ PRÁCE  
PRO OBOR MATERIÁLOVÉ VĚDY A INŽENÝRSTVÍ



BRNO 2015

## **KEYWORDS**

dislocations, plasticity, bcc metals, multiscale, thermodynamics

## **KLÍČOVÁ SLOVA**

dislokace, plasticita, bcc kovy, víceúrovňový, termodynamika

## **MÍSTO ULOŽENÍ HABILITAČNÍ PRÁCE**

Areálová knihovna Fakulty strojního inženýrství VUT v Brně

# CONTENTS

<b>AUTHOR</b>	<b>4</b>
<b>1 INTRODUCTION</b>	<b>5</b>
<b>2 ATOMISTIC STUDIES OF DISLOCATIONS</b>	<b>9</b>
2.1 Interatomic potentials and the density of states . . . . .	10
2.2 Atomistic studies of $1/2\langle 111 \rangle$ screw dislocations in BCC metals	11
2.3 Yield criterion taking into account non-glide stresses . . . . .	13
<b>3 THERMALLY ACTIVATED DISLOCATION GLIDE</b>	<b>15</b>
3.1 Thermodynamics of dislocation glide . . . . .	15
3.2 Model predictions and their correlations with experiments . . .	17
3.3 Impact of our theoretical framework . . . . .	17
3.4 Recent developments . . . . .	19
<b>4 EXPERIMENTAL STUDIES OF PLASTICITY</b>	<b>20</b>
4.1 New studies of slip traces in compressed tungsten . . . . .	20
4.2 Experiments on free-standing pillars . . . . .	23
<b>REFERENCES</b>	<b>24</b>
<b>SELECTED IMPACT PUBLICATIONS</b>	<b>29</b>
<b>ABSTRACT</b>	<b>30</b>

## AUTHOR

Name **Roman Gröger**  
Date of birth May 9, 1976  
Employer Institute of Physics of Materials, Acad. Sci.  
Czech Rep., Žižkova 22, 61669 Brno  
Telephone +420 532 290 448  
Web <http://groger.ipm.cz>  
E-mail [groger@ipm.cz](mailto:groger@ipm.cz)



### Education

2002–2007 Ph.D. (Materials Science and Engineering)  
University of Pennsylvania, USA  
2000–2003 Ph.D. (Engineering Mechanics)  
Brno University of Technology, Czech Republic  
1994–1999 Ing. (Engineering Mechanics)  
Brno University of Technology, Czech Republic

### Professional development

2014–present Research group leader (CEITEC, RG-1-11)  
2014–present Lecturer (Faculty of Mechanical Engineering, BUT)  
2012–present Secretary of the supervisory board (IPM, ASCR)  
2010–2013 Junior researcher (CEITEC, RG-1-11)  
2009–present Research scientist (Institute of Physics of Materials, ASCR)  
2007–2009 Postdoctoral fellow (Los Alamos National Laboratory, USA)  
2004–2006 Teaching assistant (University of Pennsylvania, USA)  
2000–2002 Research assistant (Institute of Physics of Materials, ASCR)  
2000–2002 Lecturer (Faculty of Mechanical Engineering, BUT)

### Awards

2010 O. Wichterle Prize (Academy of Sciences of the Czech Republic)  
2007–2009 Seaborg Fellowship (Los Alamos National Laboratory, USA)  
2007 S. J. Stein Prize (University of Pennsylvania, USA)  
1999, 2003 Rector's prize (Brno University of Technology)  
2001 Dean's prize (Faculty of Mechanical Engineering, BUT)  
1999 M.S. with honors (Faculty of Mechanical Engineering, BUT)

### Current research focus

Atomic-level studies of plasticity of bcc and hcp metals. Development of mesoscopic models of plasticity based on strain-based free energy functionals. Unraveling the origin of threading dislocations and the effect of large misfit in III-nitride semiconductor heterostructures (primarily AlN/Si). Semi-empirical description of bonding based on the theory of pseudopotentials.

# 1 INTRODUCTION

One of the biggest challenges in materials science and condensed matter physics is to link the internal structure of materials with their physical properties within a wide range of length and time scales. Due to the complexity of the problem with spanning different scales, it is often convenient to develop a hierarchy of theoretical models each of which is applicable to a certain range of scales. Many such models have been developed in the past, ranging from first principles based descriptions, via many flavors of mesoscopic models, to macroscopic models used to make engineering predictions (see Fig. 1). While each of these models may represent a more or less accurate description of the material at the scales corresponding to its domain of applicability, their predictions quickly deteriorate beyond these limits. The mismatch of predictions arising from different models is a manifestation of the break-down of the so-called *handshake paradigm* that has to be established to develop a systematic understanding of the structure-property relationships across scales.

A classical example of the coarse-graining process is the development of an interatomic potential for known reference crystal structure. The mathematical expression of the potential is obtained by intuition/experience (empirical potentials) or based partially on insight gained through more accurate schemes such as *ab initio* methods (semi-empirical potentials). Once the mathematical description of the potential is formed, it remains to determine the values of its adjustable parameters. These are obtained by fitting to experimental data and/or to results of first principles calculations.

If the functional form of the potential describes relevant aspects of the underlying physics, a small number of adjustable parameters is needed to describe the atomic environments that deviate from the reference structure. We say that the potential is transferable to other atomic environments. This transferability provides some confidence that the potential may describe correctly the energies of point defects, structures of dislocation cores, surface reconstructions, structures of grain boundaries, and the like. On the other

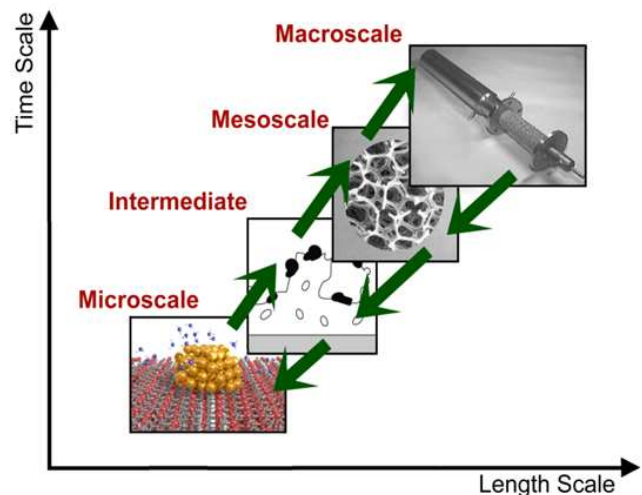


**Figure 1:** Schematic view of the multiscale hierarchy of materials modeling. Each theoretical model is applicable to a range of length and time scales beyond which its predictions should be thoroughly tested. Source: <http://essenceofscience.se/nobel-2013>

hand, if the form of the potential does not include the correct physics, many adjustable parameters are typically needed to parametrize even the reference crystal structure. It is then not surprising that those features included in the parametrization are reproduced correctly, whereas the transferability to other atomic environments is often quite poor.

The predictive value of a theory often decreases with increasing number of adjustable parameters. Perhaps a slight exaggeration will make this point clear: “If too many inputs are used to parametrize the theory, we don’t learn anything new by using it”. Similar problems are encountered at all levels of modeling. The first step is always to develop the functional form that represents the crucial aspects of the governing physics, while leaving behind a set of variables that will parametrize (or specialize) the model to a certain group of materials. These parameters are then determined using a combination of experimental measurements and lower levels of modeling, such as first principles. This process can be illustrated most straightforwardly for inert gases (group VIIIA materials), all of which have full outer electron shells. In these materials, the potential energy of a pair of interacting atoms separated by the distance  $r$  is a consequence of the competition of long-range van der Waals attraction (proportional to  $-1/r^6$ ) and short-range repulsion due to the Pauli exclusion principle ( $1/r^{12}$  term). This simple idea gave rise to the (6-12) Lennard-Jones potential,

$$V = 4\epsilon \left[ \left( \frac{\sigma}{r} \right)^{12} - \left( \frac{\sigma}{r} \right)^6 \right], \quad (1)$$

where  $\epsilon$  and  $\sigma$  set the energy and length scales, respectively. Owing to the correct physics embodied in the mathematical form of this potential, it has been shown to reproduce accurately a wide range of physical properties of inert gases.

However, this formulation is not applicable to ionic materials (e.g. NaCl), covalent solids (e.g. semiconductors such as Si or Ge), metals and semi-metals, and to materials with mixed bonding (metallic-covalent, covalent-ionic). Different descriptions of bonding have been developed for these materials that are based on a simple electrostatic interaction (ionic materials), Embedded Atom Method (EAM) and Modified Embedded Atom Method (MEAM) potentials (metals), Tersoff potential (semiconductors), Tersoff-Brenner potential (covalent-ionic solids), and semi-empirical Bond Order Potentials (BOP) and Modified Generalized Pseudopotential Theory (MGPT) (covalent-metallic bonding). The development of interatomic potentials is sometimes more of an art than a science and often requires inputs from first principles (quantum-mechanical) calculations.

While atomistic simulations using empirical and semi-empirical potentials have been indispensable to gain insight into the internal structure of nanoma-

materials and nanosized defects, they are not practical (and sometimes possible) for large systems. One obvious limitation is the available computational power. However, a much less accented drawback of these models is that all degrees of freedom are taken at the same footing. For example, if we study a network of dislocations, most of the atoms are displaced by the superposition of linear-elastic strain fields of all dislocation segments, while only a small fraction corresponds to dislocation cores. This suggests to subdivide the simulation domain into two regions: (i) atomistic region, where the positions of atoms are determined by the interatomic potential, and (ii) the region between defects, which can be described using continuum methods. This approximation is employed in the Quasicontinuum method ([qcmethod.org](http://qcmethod.org)) developed originally by Ellad Tadmor (U. Minnesota) and Rob Phillips (Caltech). Another possible coarse-graining scheme is to represent the dislocation cores by a series of piecewise linear segments whose interaction is assumed to be governed by linear elasticity. This concept was developed by Kubin et al. and originally implemented in the code `Micromégas`; for a recent review, see the book of Kubin [47]. Among the most widely used implementation of this Discrete Dislocation Dynamics (DDD) method is the ParaDiS code ([paradis.stanford.edu](http://paradis.stanford.edu)) developed at the Lawrence Livermore National Laboratory (LLNL). Our work mentioned further in this text used the code developed by Daniel Weygand at Karlsruhe Institute of Technology.

The transition between different scales is often made quite abrupt by adopting a different theoretical description. This is most evident when going from atomistic models that are based on the positions and momenta of particles to mesoscopic models formulated using continuous fields. One of the latter examples is the Landau-Ginzburg theory which has been immensely successful at predicting the microstructural changes in materials undergoing structural phase transitions. It replaces the discrete view of the crystalline lattice by smooth order parameter fields and the interatomic potential by the free energy functional formulated in terms of these fields. Although there are only three adjustable parameters needed to describe the first-order cubic-to-tetragonal phase transition (four if the lowest order gradient of the order parameter is considered), this theory can describe self-organizations and phase transitions in materials at the length scales down to a few atomic unit cells and up to macroscopic length scales [44]. Similar mesoscopic theories have provided great insights into many diverse critical phenomena, such as superconductivity [23], ferroelectricity [11], damping in ferromagnetic materials [22] and twinning [3].

In a similar spirit, Langer [48] formulated a continuum model that can be used to model interfaces between different materials. This gave rise to the phase field crystal (PFC) model, which has been applied successfully to the studies of viscosity, evolution of fracture, dynamics of vesicles, and others [60].



The field-theoretical approach of Landau is unique in the sense that it describes a wide range of scales using a single mathematical formula. Another representative of this class is the block scaling proposed by Kadanoff in 1966. This was further developed into the renormalization group theory by Wilson for which he received the 1982 Nobel Prize in Physics; for a popular presentation, see [77]. Instead of choosing a different theoretical description of the problem when changing the scale, the mathematical form is kept fixed and the adjustable parameters (coupling constants) are varied. For example, consider the ferromagnetic Ising model defined by the Hamiltonian

$$H = -J \sum_{\langle ij \rangle} s_i s_j , \quad (2)$$

where  $s_i = \pm 1$  are the up/down spins, respectively. When passing to larger scales, the individual spins are grouped into blocks and replaced by “block spins” [77]. Since the mathematical form of the Hamiltonian remains fixed, the coupling constant  $J$  has to be renormalized so as to represent different interactions of these block spins. Repeating this process brings the system through many length scales to the point where only one spin remains. The coarse-graining process is thus viewed as a flow of the coupling constant,  $J(\phi) \rightarrow J(\phi')$ , where  $\phi$  and  $\phi'$  represent two successive scales. The snapshots of the system taken at different scales represent possible realizations of the system at these scales. The results of this scaling are critical fixed points (stable or unstable) that represent the macroscopic properties of the system. The stable fixed point determines the properties of the system at high temperatures, where the microstructure is spatially disordered (i.e. the correlation length is zero). On the contrary, the unstable fixed point describes the behavior of the system near the critical temperature ( $T = 0$  K), where the correlation length diverges. This is the key observation that allows to sort seemingly unrelated systems into a finite number of universality classes, where each class includes systems with the same critical behavior. While many other renormalization group transformations have been developed over the years, there are some in which divergences present at small scales proliferate through all length scales and thus the model becomes nonrenormalizable [69].

There are many theoretical and experimental studies that investigate scaling phenomena in crystal plasticity. However, it is often quite difficult to determine the corresponding universality class because the glide of dislocations is an inherently rare, thermally activated event. While this problem can be to some extent circumvented by artificially increasing the applied load (or increasing temperature), these changes are not easily accepted because they may alter the behavior of the system. The correct approach would be to use large systems and study their behavior over long time scales to acquire good

statistics and determine the scaling exponents. This has been accomplished recently by Tsekenis et al. [73], who showed that the critical behavior of the interacting system of parallel edge dislocations belongs to the same universality class as the mean-field interface depinning model.

It should be evident from above that there are two distinct approaches to developing multiscale models of any kind. One is based on formulating a hierarchy of models, where each represents only a certain range of scales. The problem with these models is that their predictions often do not match at intermediate scales. The second approach is to construct a single theoretical model and vary (renormalize) their adjustable parameters so as to bring the system through a wide range of scales. The former is often adopted by researchers who view the problems from the discrete perspective, i.e. they model the material as a collection of interacting atoms with perhaps an underlying electronic structure. On the other hand, the renormalization methods are the workhorse of field theorists. The importance of these methods in materials science was demonstrated by Goldenfeld [25].

The purpose of this thesis is to summarize our past bottom-up developments of the multiscale theory of plasticity of body-centered cubic (BCC) metals. These have been made during my Ph.D. study at the University of Pennsylvania (2002-2007), my postdoctoral fellowship at the Los Alamos National Laboratory (2007-2009), and continue to be at the forefront of my research at the Institute of Physics of Materials of the Academy of Sciences of the Czech Republic and the Central European Institute of Technology (CEITEC) (2009-present). The first part of this document is focused on gaining a deep insight into the properties of isolated  $1/2\langle 111 \rangle$  screw dislocations in BCC metals and representing these results mathematically using a relatively simple form of an effective yield criterion. Both atomistic results and the yield criterion are then employed to construct a thermodynamic model of slip whose predictions can be correlated with experiments to verify the accuracy of this multiscale framework. Besides our previous work, I briefly introduce our current efforts and outline the most interesting problems that remain at the top of our to-do list for the near future.

## 2 ATOMISTIC STUDIES OF DISLOCATIONS

Since the work of Taylor and Elam [71, 72], the plastic deformation of BCC metals has been known to be very different from that of close-packed metals such as Cu or Au, which are often used to explain plasticity in undergraduate courses. Moreover, BCC metals (now primarily W and  $\alpha$ -Fe) are promising materials for use as plasma divertors in nuclear fusion power plants. The purpose of this section is to provide a brief historical account of the most

important descriptions of atomic interactions in these materials. A large part of this section summarizes our recent atomistic studies of the structure and properties of  $1/2\langle 111 \rangle$  screw dislocations in BCC metals.

## 2.1 Interatomic potentials and the density of states

It was proposed already by Friedel [20] that the strength of bonding is intimately linked with the density of states. The number of moments needed to be employed in the description of atomic interactions depends on the complexity (curvature) of the density of states. This is rather simple for materials with nearly free (or nearly full) outer electron shells, such as simple metals of the group I and II and face-centered cubic (FCC) metals Cu, Au or Al. All these materials have almost flat density of states near the Fermi energy and thus the second moment approximation of the density of states suffices to describe bonding in these materials. This approximation is at the core of all potentials of the Embedded Atom Method (EAM) family [10] that are widely used to carry out molecular simulations of both elemental metals and alloys.

The second moment approximation of the density of states treats each material in the nearly-free electron approximation, i.e. as if the bonding was purely metallic. This is not the case in refractory metals, where the density of states has a bimodal character and, therefore, the bonding is partially covalent and partially metallic. Nevertheless, there have been early attempts to extend the second moment approximation of the density of states also to refractory BCC metals [1]. These provided important qualitative insights into the structure and stability of dislocations in these materials [15, 16, 18, 42]. However, the presence of the drop in the density of states near the Fermi energy calls for potentials that employ higher moments of the density of states.

One such approach, that was developed around the 1990s at the University of Oxford, is based on the tight binding formalism of Pettifor [59] and uses the concept of bond order to describe directional many-body interactions in transition metals. This scheme was successfully employed to develop accurate semi-empirical potentials for Ti and TiAl [24, 78], which were followed by potentials for Mo [54, 56], Mo-Si [9, 54], Ir [9] and, with my partial contribution, also for W [55]. The most recent contribution to this field was the development of BOPs for all refractory metals [50] which substantially speed up the minimization of energy (molecular statics) and numerical integrations of the equations of motion (molecular dynamics).

The importance of BOPs stems from the fact that they are derived self-consistently by coarse-graining the electronic structure within the tight-binding formalism [40]. Keeping this link not only allows their accurate parametrizations using first principles data but it also guarantees that the potential is transferable to quite different atomic environments than the reference BCC

structure. Indeed, this transferability has been demonstrated for all refractory metals and  $\alpha$ -Fe by calculating the energies of crystals deformed along characteristic transformation pathways (tetragonal, orthorhombic, hexagonal, trigonal) and comparing these with first-principles data. All calculations on BCC metals discussed in the following text were made using these BOPs.

## 2.2 Atomistic studies of $1/2\langle 111 \rangle$ screw dislocations in BCC metals

The early studies of the structure and energetics of isolated  $1/2\langle 111 \rangle$  screw dislocations using the BOP for Mo were published in Ref. [75]. Here, we determined how pure shear stress parallel to the slip direction acting in a range of the so-called maximum resolved shear stress planes (MRSSP) of the  $[111]$  zone depends on the angle  $\chi$  between the MRSSP and the  $(\bar{1}01)$  plane that is the most highly stressed  $\{110\}$  plane of the  $[111]$  zone. The critical stress to move the dislocation, the so-called critical resolved shear stress (CRSS), was shown to depend on the orientation of the MRSSP. This violates the predictions of the Schmid law [67], which asserts that  $\text{CRSS} \propto 1/\cos \chi$ , i.e. that  $\text{CRSS}(\chi)$  is symmetric about  $\chi = 0$ . In particular, for Mo, it is shown to increase steeply for positive  $\chi$  but more steadily for negative  $\chi$ . This twinning-antitwinning asymmetry has been known for a long time [35] but its origin was not known. Our calculations revealed that this twinning-antitwinning asymmetry is a property of a single dislocation and it is a direct consequence of the shear stresses that are parallel to the slip direction but acting in planes other than the most highly stressed  $(\bar{1}01)$  plane (the so-called *non-glide stresses*).

In parallel, we have developed a simple theoretical argument which may explain the factor of 2 to 3 (sometimes even 4) discrepancy between the calculated CRSS and the experimentally measured yield stresses [30]. This discrepancy is shown to disappear if one takes into account the interactions between dislocations ahead of the Frank-Read source. Such a view is consistent with previous experiments made on BCC metals by Louchet [51], which suggest that the plastic deformation of these materials is governed by screw dislocations moving in groups. Interestingly, no such collective motion of dislocations is observed in recent in situ TEM studies of Caillard [8] on  $\alpha$ -Fe. At the time, it is not clear what fraction of the above-mentioned yield stress discrepancy can be attributed to the presence of magnetism in  $\alpha$ -Fe and what part is inherent to the BCC crystal structure. More recently, Proville, Rodney et al. [4, 61] have argued that the origin of this discrepancy in materials with large Debye temperatures (such as BCC metals) can be the neglect of quantum zero-point motion of atoms. While this leads to some reduction of the yield stress, their model does not explain how random oscillations of atoms lead to the collective motion of many atoms in the activated segment of the dislocation. The origin of this discrepancy thus remains elusive.

Further work focused on investigating the role of shear stresses perpendicular to the slip direction. Their importance was predicted already by Duesbery [15] and investigated to some extent using the Finnis-Sinclair potential for Mo and Ta [1] by Ito and Vitek [42]. This stress component does not exert any Peach-Koehler force on the dislocation and the dependence of the CRSS on this stress component was initially quite surprising. In our work, we define this load by the stress tensor

$$\Sigma^\tau = \begin{bmatrix} -\tau & 0 & 0 \\ 0 & \tau & 0 \\ 0 & 0 & 0 \end{bmatrix}, \quad (3)$$

where  $\tau$  imposes the shear stress perpendicular to the slip direction. We have demonstrated [28] that these stresses modify the structure of the dislocation core and thus promote the slip on that  $\{110\}$  plane into which the core is predominantly extended. This is shown in Figs. 2a,b for negative and positive applied shear stresses perpendicular to the slip direction ( $\tau$ ), respectively, where the “+” signs represent extensions and the “-” signs contractions of the dislocation core. For positive  $\tau$  (Fig. 2b), the dislocation core extends on the most highly stressed ( $\bar{1}01$ ) plane. The dislocation then moves preferentially by normal slip on this ( $\bar{1}01$ ) plane. Negative shear stresses  $\tau$  (Fig. 2a) extend the dislocation core into one of the two low-stressed planes, either ( $0\bar{1}1$ ) or ( $\bar{1}10$ ). When the shear stress parallel to the slip direction reaches the CRSS, the dislocation moves on one of these planes despite the fact that they have low Schmid factors. This is the mechanism of the so-called *anomalous slip*, which is predicted by these atomistic simulations to occur only in compression, where the shear stress perpendicular to the slip direction is negative.

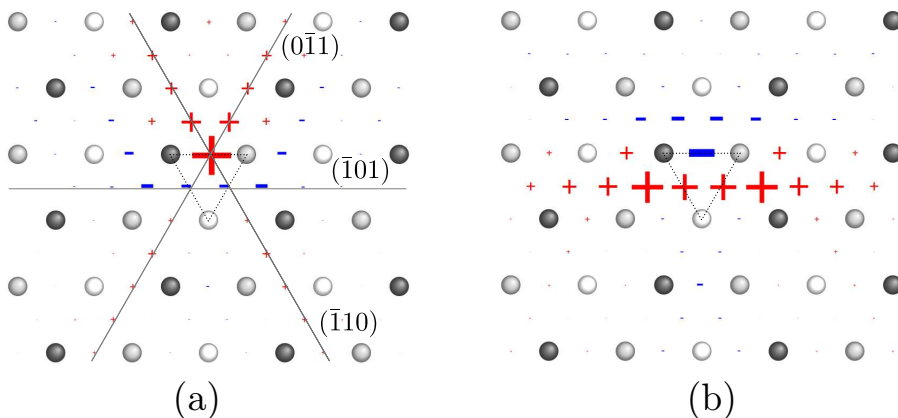


**Figure 2:** Difference plots showing the changes in the core structure of a  $1/2[111]$  screw dislocation in BCC metals relative to the unstressed crystal. Here, (a) corresponds to negative and (b) to positive applied shear stresses perpendicular to the slip direction ( $\tau$ ) applied using the stress tensor (3). There is a clear extension of the dislocation along ( $0\bar{1}1$ ) and ( $\bar{1}10$ ) planes in (a) and on the ( $\bar{1}01$ ) plane in (b).

The anomalous slip was observed originally in Nb [7, 17]. Since then, it has been encountered in almost all BCC transition metals with the exception of  $\alpha$ -Fe and Cr, where magnetism is believed to suppress core transformations. Our results imply that the anomalous slip is a property of a single  $1/2\langle 111 \rangle$  screw dislocation and occurs as a consequence of core transformations induced by the shear stress perpendicular to the slip direction. This view has been recently challenged by Marichal et al. [52] who argue that the anomalous slip is not the property of a single dislocation but occurs as a consequence of interactions of screw dislocations in two  $\{110\}\langle 111 \rangle$  systems with the highest Schmid factors. However, the activity of the low-stressed system in their work is quite weak because it contributes only 9% to the total plastic strain. This provides some evidence that the mechanism studied in their work may not be the anomalous slip observed originally by Duesbery [14] and Bolton & Taylor [7] but, instead, normal slip on the two most highly stressed systems. Apparently, the origin of the anomalous slip is still far from being understood and it seems to attract renewed interest [41, 52]. It should be also emphasized that the anomalous slip is not specific to BCC metals but is frequently encountered also in hexagonal metals deforming by non-basal slip in conjunction with pronounced twinning.

### 2.3 Yield criterion taking into account non-glide stresses

The dependence of the CRSS on the two kinds of non-Schmid (or non-glide) stresses above suggests that the onset of plasticity in BCC metals cannot be described by a simple flow rule such as those formulated by von Mises or Tresca [38], as it is common in close-packed metals. Instead, the von Mises equivalent stress or Tresca's stress intensity represent only one contribution to the effective stress, whereas the dependence of the CRSS on the orientation of the MRSSP and the effects of shear stresses perpendicular to the slip direction need to be accommodated using additional terms.

One of the simplest ways to accomplish this was the approach suggested by Qin and Bassani [63, 64] which was originally applied to L1<sub>2</sub> intermetallics, in particular Ni<sub>3</sub>Al. We have used this methodology to develop a yield criterion for single crystals of BCC metals, in which the effective yield stress ( $\tau^{*\alpha}$ ) for each slip system  $\alpha = 1 \dots 24$  depends linearly on the Schmid stress and three non-glide stresses,

$$\tau^{*\alpha} = \tau_0^\alpha + a_1\tau_1^\alpha + a_2\tau_2^\alpha + a_3\tau_3^\alpha \leq \tau_{cr}^{*\alpha} . \quad (4)$$

If the orientation of the crystal is  $x = [\bar{1}2\bar{1}]$ ,  $y = [\bar{1}01]$  and  $z = [111]$ , the stress component  $\tau_0^\alpha = \mathbf{m}^\alpha \boldsymbol{\Sigma}^c \mathbf{n}^\alpha$  is the Schmid stress  $\sigma_{23}^{(\bar{1}01)}$ ,  $\tau_1^\alpha = \mathbf{m}^\alpha \boldsymbol{\Sigma}^c \mathbf{n}_1^\alpha$  the shear stress  $\sigma_{23}^{(0\bar{1}1)}$  parallel to the slip direction acting in the  $(0\bar{1}1)$  plane,  $\tau_2^\alpha = (\mathbf{n}^\alpha \times \mathbf{m}^\alpha) \boldsymbol{\Sigma}^c \mathbf{n}^\alpha$  the shear stress  $\sigma_{12}^{(\bar{1}01)}$  perpendicular to the slip direction

acting in the  $(\bar{1}01)$  plane and  $\tau_3^\alpha = (\mathbf{n}_1^\alpha \times \mathbf{m}^\alpha) \Sigma^c \mathbf{n}_1^\alpha$  the shear stress  $\sigma_{12}^{(0\bar{1}1)}$  perpendicular to the slip direction acting in the  $(0\bar{1}1)$  plane. Here,  $\Sigma^c$  is the stress tensor expressed in the  $\langle 100 \rangle$  cube orientation,  $\mathbf{m}^\alpha$  the unit vector parallel to the slip direction,  $\mathbf{n}^\alpha$  the unit vector perpendicular to the slip plane, and  $\mathbf{n}_1^\alpha$  the unit vector perpendicular to the non-glide plane in zone of the slip direction  $\mathbf{m}^\alpha$ . The coefficients  $a_1, a_2, a_3$  and the yield stress  $\tau_{cr}^*$  are parametrized using the results of atomistic simulations [29].

The tensorial form (4) is particularly useful for predicting the onset of slip activity of all 24 slip systems in BCC metals. For loading in tension, the calculations made on Mo and W predict that the slip occurs primarily on the  $(\bar{1}01)[111]$  system that has the highest Schmid factor (yellow region in Fig. 3a). However, the predictions are very different in compression for both these metals, as shown in Fig. 3b for Mo and in Fig. 3c for W. In the former, there is a large region of slip activity on the system  $(\bar{1}01)[\bar{1}\bar{1}\bar{1}]$  (yellow), which has the highest Schmid stress in compression. However, the primary slip system for W predicted for a wide range of orientations within the standard stereographic triangle is  $(\bar{1}10)[\bar{1}\bar{1}\bar{1}]$  (blue). This is one of the two  $\{110\}$  slip systems of the  $[\bar{1}\bar{1}\bar{1}]$  zone into which the dislocation can cross-slip, and its Schmid factor is typically around a half of that for the  $(\bar{1}01)[\bar{1}\bar{1}\bar{1}]$  system. These results support our earlier argument that the anomalous slip is predicted to occur in both Mo and W but only in compression. Unlike Mo, where it is operative only for loading directions close to the  $[001]$  corner and

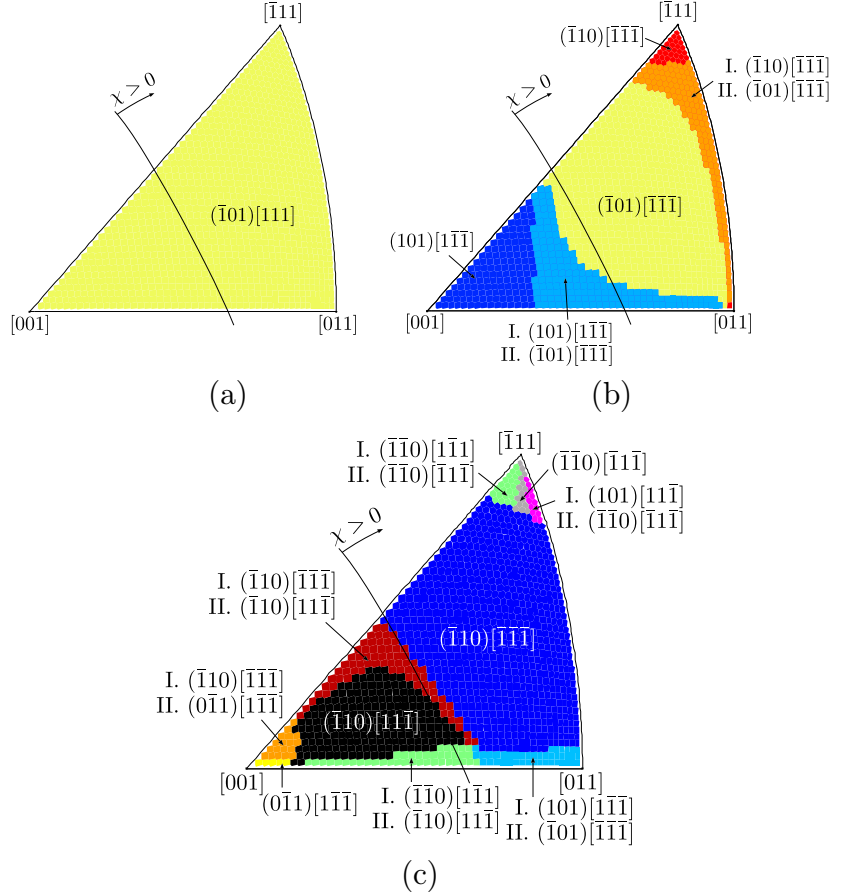


**Figure 3:** Slip activity in Mo and W predicted by the yield criteria developed in Refs. [28] and [29]. The figure (a) corresponds to loading in tension (both Mo and W), (b) to compression in Mo, and (c) to compression in W. Each point in these stereographic triangles represents a different loading direction and colors distinguish the regions of different slip activity.

where it is operative only for loading directions close to the  $[001]$  corner and

the [011]- $\bar{[111]}$  edge of the stereographic triangle, it seems to be dominant for a broad range of orientations in W.

While for Mo we observed a very good agreement of our theoretical predictions with experiments, there are much fewer measurements that could be used for W [2, 21, 45, 66]. There is a clear need for more experiments that will identify the order of activation of individual slip systems. The most promising ongoing experiments together with our recent efforts to fill this gap will be presented in Section 4.

### 3 THERMALLY ACTIVATED DISLOCATION GLIDE

In order to extend the atomistic results to finite temperatures and plastic strain rates, one has to develop a thermodynamic model of slip in these materials. A particularly useful approach to do that is the variational formulation developed by Dorn and Rajnak [13], where they consider that the dislocation is confined to move in a single (and known) slip plane. As our previous atomistic simulations show, this is not the case for BCC Mo and W and, therefore, an extension of this model was needed to allow for cross-slip of these dislocations. A similar framework will be needed for all materials in which the plastic flow is not governed by the Schmid law.

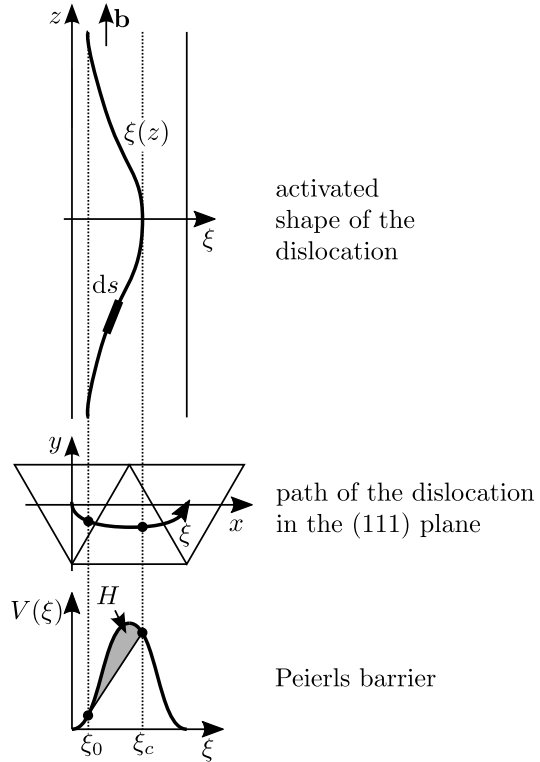
#### 3.1 Thermodynamics of dislocation glide

We have generalized the formalism in Ref. [13] as follows (for details, see Ref. [31]). Firstly, we consider that the  $1/2[111]$  screw dislocation is a straight line that is parallel to the  $z$  direction and its intersection with the perpendicular (111) plane is the point  $[x_0, y_0]$ . It is convenient to define the shape of the dislocation line parametrically as  $\xi(z) = [x(z), y(z)]$ , i.e. the position of the straight dislocation is denoted as  $\xi_0 = [x_0, y_0]$ . The line energy of the straight dislocation is then  $E_0 = \int_{-\infty}^{\infty} V(\xi_0) dz$ , where  $V$  is the two-dimensional Peierls potential, defined in the (111) plane, that opposes the dislocation glide. We consider that the endpoints of the dislocation are fixed and thus the dislocation moves by bowing out a part of its length into the direction of the applied shear  $\sigma$ . For an arbitrary shape of the dislocation,  $\xi(z)$ , its associated line energy can be written as  $E = \int_{-\infty}^{\infty} V[\xi(z)] ds$ , where  $ds = \sqrt{dx^2 + dy^2 + dz^2}$ . Finally, the work done by the applied stress during the transformation of the shape of the dislocation from  $\xi_0$  to  $\xi(z)$  is  $W(\sigma) = \sigma b \int_{-\infty}^{\infty} [\xi(z) - \xi_0] dz$ . The activation enthalpy to move the dislocation is defined as  $H(\sigma) = E - E_0 - W(\sigma)$ , which can be easily put into the following form

$$H(\sigma) = \int_{-\infty}^{\infty} \left\{ V[\xi(z)] \sqrt{1 + [\xi'(z)]^2} - V(\xi_0) - \sigma b [\xi(z) - \xi_0] \right\} dz, \quad (5)$$



**Figure 4:** Schematic illustration of the activated shape of the dislocation at a finite applied shear stress  $\sigma$ . The middle panel shows a curved transition pathway of the dislocation between two potential minima in the (111) plane. This is calculated, for example, using the Nudged Elastic Band (NEB) method. The lower panel shows the Peierls barrier along this curved path. The activated shape of the dislocation is a three-dimensional curve between the positions  $\xi_0$  and  $\xi_c$  along this curved path. The activation enthalpy corresponds to the area between the Peierls barrier and its tangent at the point  $\xi_0$  (gray).



where we have used the identity  $d\xi^2 = dx^2 + dy^2$ .

We are looking for the shape of the dislocation,  $\xi(z) = [x(z), y(z)]$ , that corresponds to the minimum of the activation enthalpy  $H(\sigma)$  for the given applied shear stress  $\sigma$ . Recognizing that the activation enthalpy (5) is of the form  $H = \int_{-\infty}^{\infty} L[\xi(z), \xi'(z)] dz$  and since the integrand  $L[\xi(z), \xi'(z)]$  does not depend explicitly on  $z$ , the associated Euler-Lagrange equation reduces to the Beltrami identity, which is an autonomous ordinary differential equation. The slope of the dislocation,  $\xi'(z)$ , is obtained by direct integration with the Dirichlet boundary conditions  $\xi(\pm\infty) = \xi_0$  and  $\xi(0) = \xi_c$ . Here,  $\xi_0$  is the position of a *straight* dislocation at the stress  $\sigma$  and  $T = 0$  K. This is obtained from  $\sigma b = (dV/d\xi)_{\xi=\xi_0}$ . The limit  $\xi_c$  also corresponds to the position of a straight dislocation, but obtained from the condition of vanishing activation enthalpy (5). This is defined implicitly as  $V(\xi_c) - V(\xi_0) = \sigma b(\xi_c - \xi_0)$ . Upon employing the slope of the dislocation back in (5) and changing the integration variable, we obtained the following expression for the stress dependence of the activation enthalpy:

$$H(\sigma) = 2 \int_{\xi_0}^{\xi_c} \sqrt{[V(\xi)]^2 - [\sigma b(\xi - \xi_0) + V(\xi_0)]^2} d\xi. \quad (6)$$

Here,  $\xi_0$  and  $\xi_c$  define the range of positions along the curved path of the dislocation  $\xi$  traced by all segments of the activated dislocation, and  $V(\xi)$  is the Peierls barrier that represents a cross-section of the two-dimensional Peierls potential along the curved dislocation path. The Peierls potential is a

theoretical concept that quantifies the changes of the dislocation line energy as the dislocation moves through the crystal.

It is important to emphasize that the concept of the Peierls barrier is not as simple as, for example, the migration barrier of point defects. While the latter affects the kinetics of diffusion of point defects only through the energy difference  $\Delta E$  between the initial and maximum-energy configurations along the migration path, the whole shape of the Peierls barrier is needed to determine the activation enthalpy (6) and its dependence on the applied stress. Therefore, the shape of the Peierls barrier  $V(\xi)$  is considered to be a function of non-glide stresses, whereas the dislocation overcomes this barrier by the action of the Schmid stress.

### 3.2 Model predictions and their correlations with experiments

In principle, (6) can be used to obtain the stress dependence of the activation enthalpy for any applied stress. This nevertheless relies heavily on two ingredients: (i) knowledge of the minimum energy path of the dislocation  $\xi(z)$  in the perpendicular (111) plane between the two positions in the lattice represented by  $\xi_0$  and  $\xi_c$ , and (ii) the associated Peierls barrier  $V(\xi)$ .

In our previous work [31], we have constructed the Peierls barrier empirically based on the suggestion of Edagawa et al. [19], where an additional distortion of the maxima had to be introduced to reproduce the curvature of the temperature dependence of the flow stress (originally suggested by Suzuki et al. [70]). The minimum energy path  $\xi(z)$  was then calculated by employing the Nudged Elastic Band (NEB) method [37, 43].

Knowing  $H(\sigma)$ , the temperature dependence of the flow stress was obtained using the Arrhenius law  $\dot{\gamma} = \dot{\gamma}_0 \exp[-H(\sigma_f)/kT]$ , where  $k$  is the Boltzmann constant and  $\sigma_f$  the flow stress (it coincides with the yield stress  $\sigma$  for  $T = 0$  K and quasistatic loading). For typical engineering conditions, this means that  $H(\sigma_f) = (20 \dots 40)kT$ , which can be inverted numerically to arrive at  $\sigma_f(T, \dot{\gamma})$ . This thermodynamic model predicted for the first time both the temperature and strain rate dependencies of the yield stress in Mo and W at low temperatures (Fig. 5). Simultaneously, the model reproduces the complex character of the tension-compression asymmetry in these materials [26].

### 3.3 Impact of our theoretical framework

Our theoretical model was quickly picked up by the group of Peter Gumbsch at the Karlsruhe Institute of Technology to develop a discrete dislocation dynamics model for BCC metals [68]. This model is now one of the most attractive tools used to investigate plasticity of these materials at mesoscopic length scales (see also [52]).

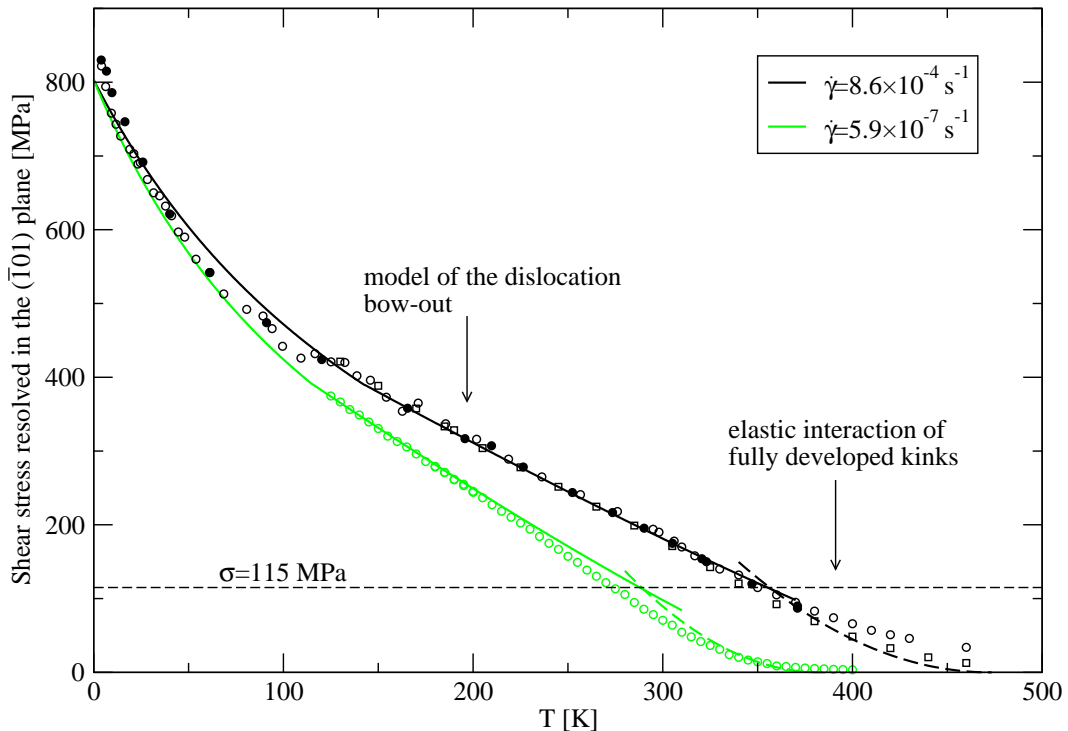


**Figure 5:** Temperature dependence of the flow stress in Mo for loading in tension along  $[\bar{1}49]$  (approx. in the middle of the stereographic triangle). The symbols are data obtained from macroscopic tensile tests of Hollang et al. [39] and the curves are predictions of our thermodynamic model outlined here. Data for two different strain rates are shown to demonstrate the accuracy of our theoretical model for a range of loading conditions. The part of the curve labeled “model of dislocation bow-out” corresponds to the model outlined here. The minor part “elastic interaction of fully developed kinks” is explained in Ref. [31].

In recent years, there were several attempts to develop crystal plasticity finite element models (CPFEM) of BCC metals based on the results of our atomistic simulations and the activation enthalpies obtained from our thermodynamic model. In particular, Weinberger et al. [76] used our effective yield criteria [29] to study the large-scale (grain size) response of Mo and W. Lim et al. [49] further extended this model by adding additional terms into the yield criterion (not present in [29]) that were thought to be missing in our work. Their argument is based on the work of Koester et al. [46], who suggest that also normal stresses affect the onset of glide of isolated screw dislocations in BCC metals (in their case  $\alpha$ -Fe). However, already the work of Duesbery [15] implies that their conclusions cannot be correct. This is demonstrated clearly in Ref. [27], where I show that the CRSS does not depend on the component  $\sigma_{33}$  that is parallel to the dislocation line. Moreover, the effect of the remaining two normal stresses,  $\sigma_{11}$  and  $\sigma_{22}$ , in the plane perpendicular to the dislocation line arises as a consequence of the shear stresses that are already included in our effective yield criterion. The extra terms in Refs. [46] and [49] are thus redundant. On the other hand, the paper of Weinberger et al. [76] may be taken as a starting point for the development of macroscopic CPFEM models

for random and textured polycrystals. The first step in this direction was made already by us [31] and was extended further by Bassani and Racherla [5].

### 3.4 Recent developments

In principle, the Peierls barrier can be obtained using the NEB method [36, 37, 43]. These calculations were indeed made in Refs. [12, 31, 62, 65, 74]. However, we have shown in Ref. [32] that a straightforward application of the NEB method to all degrees of freedom (DOF) in the crystal leads to clustering of the states of the system towards potential minima, which also overestimates the Peierls stress to move the dislocation.

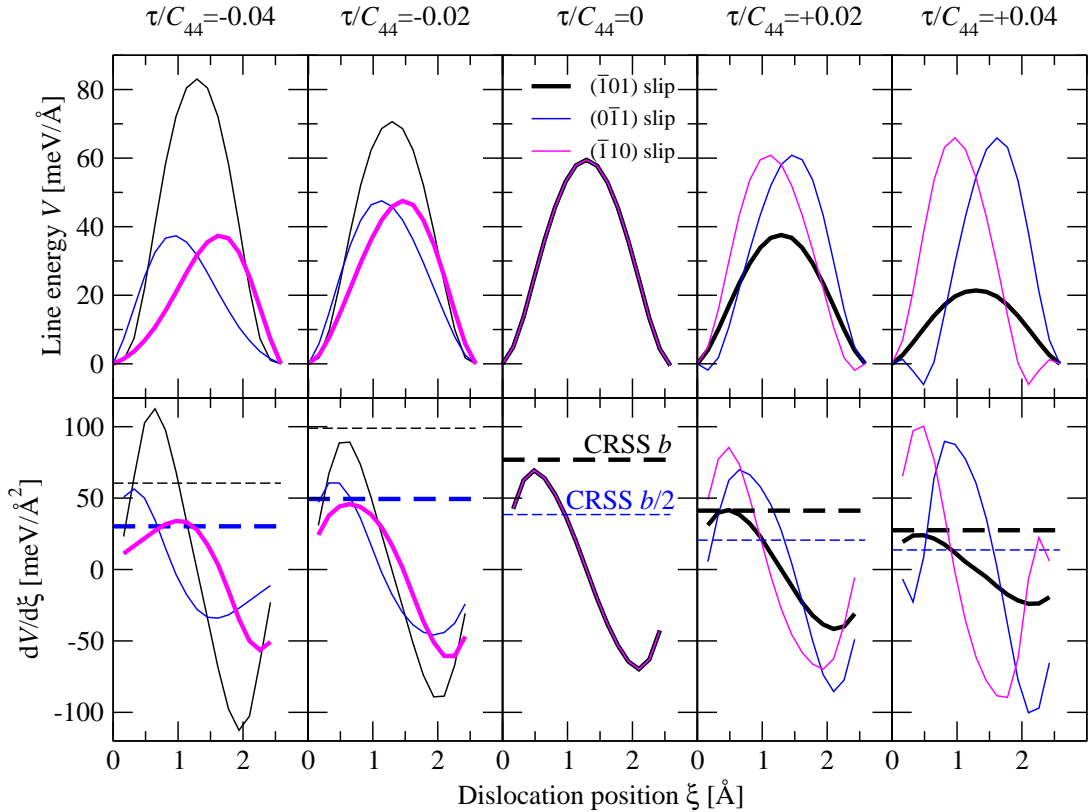


**Figure 6:** Dependence of the Peierls barrier of an isolated  $1/2[111]$  screw dislocation in W calculated by the NEB+r method [32] on the shear stress perpendicular to the slip direction ( $\tau$ ). The colors correspond to the three possible slip planes of this dislocation shown in the legend. The lower panels show the derivatives of these barriers (curves) along the minimum energy paths. The horizontal lines are predictions of  $\max(dV/d\xi)$  obtained by direct application of stress in molecular statics simulations.

In the paper [32], we suggest an elegant solution that uses the NEB method only for a limited number of DOF around the dislocation, while all other DOF are relaxed by the interatomic potential. This procedure has two significant advantages. Firstly, it introduces atomic relaxations into the calculation of the energy barrier. The second is that it avoids clustering of the dislocation positions into the nearest minimum energy configurations at the beginning and

end of the transition pathway. Interestingly, the Peierls stress determined by differentiating the Peierls barrier obtained from this new NEB+r method deviates only 8% from its value obtained by direct molecular statics calculations. We have used this method to calculate the shape of the Peierls barrier and its changes under the two non-glide stresses identified above when the MRSSP is the  $(\bar{1}01)$  plane [33]. These are the shear stresses parallel to the slip direction acting in different  $\{110\}$  planes of the  $[111]$  zone than the most highly stressed  $(\bar{1}01)$  plane, and (ii) shear stresses perpendicular to the slip direction. These results are reproduced for W in Fig. 6, where the upper panels show the Peierls barriers for the glide of the dislocation on the three  $\{110\}$  planes and the four values of the shear stresses perpendicular to the slip direction ( $\tau$ ). The lower panels are then derivatives of these barriers along the dislocation pathway ( $\xi$ ). Similar calculations are now under way for a number of other orientations of the MRSSP and for all BCC metals of the VB and VIB groups.

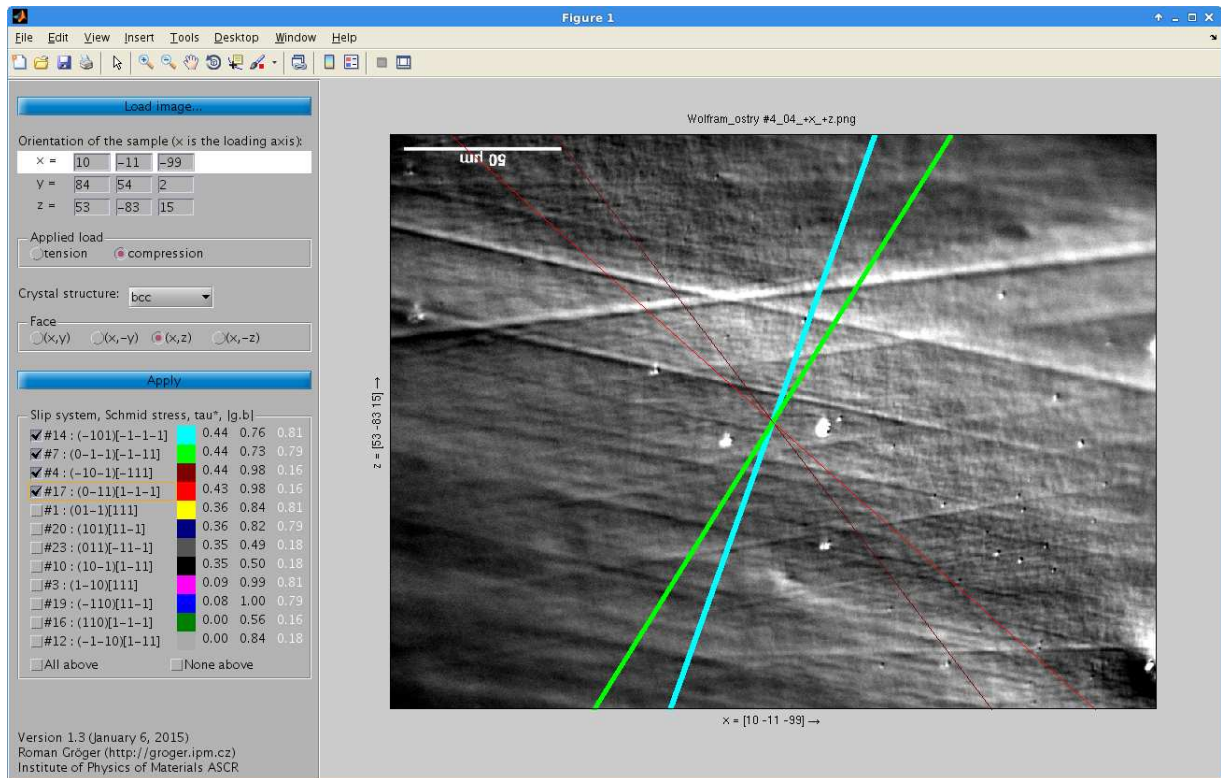
Further improvement of the accuracy of the Peierls barrier is only possible by accounting for curvature of the transition path of the dislocation between the neighboring minimum energy configurations in the lattice. There have been some models proposed by the French group that purport to account for these details [12, 65, 74]. However, all these are based either on purely geometrical arguments or on a combination of geometry with linear elasticity, without explicitly accounting for the nonlinear reconstructions of the dislocation cores. Recently, we have formulated a very different approach to identify the curved transition pathway, which is based directly on the displacements of atoms around the dislocation core [34]. This model is similar to the Peierls-Nabarro model [57, 58], but takes into account the fact that the dislocation can move on any of the three  $\{110\}$  planes in the  $[111]$  zone.

## 4 EXPERIMENTAL STUDIES OF PLASTICITY

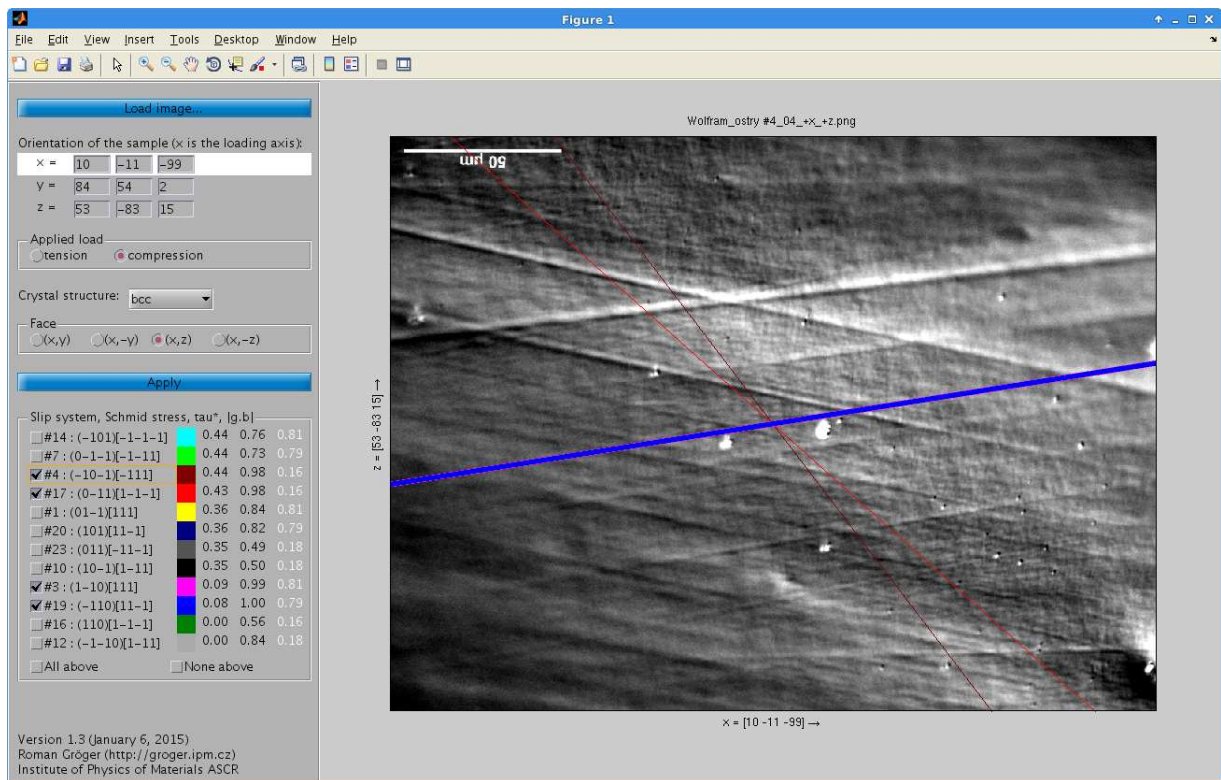
Virtually all studies of slip traces in W under stress stopped around the 1970s, which makes it one of the least studied structural materials of high technological importance. This is also one of the few materials for which experimental work starts to seriously lag behind the computational studies.

### 4.1 New studies of slip traces in compressed tungsten

About a year ago, we have started a small experimental program at IPM that combines high-precision testing of W single crystals in compression with optical and electron microscopy and computer simulations to elucidate the puzzling mechanism of plasticity in this material. The high purity tungsten single crystals were obtained by electron beam floating zone method in the group of



(a)



(b)

**Figure 7:** Comparison of the slip traces on the side A of sample #4 compressed to 4.4% plastic strain (Nomarski contrast, figure in the background) with theoretical predictions (lines in the foreground): (a) prediction of the Schmid law, (b) prediction of the  $\tau^*$  criterion developed in Refs. [28, 29]. The applied load is parallel to the horizontal axis.

Vadim Glebovsky at the Center for Scientific Research “Chernogolovka” and purchased by us through Calipso BV in Eindhoven. A large piece of metal was cut into near center-triangle orientation by spark erosion and polished. The EBSD analysis of the sample has provided the orientation of the sample, which is  $[10\bar{11}99]$ . The sample had a nearly tetragonal geometry with the length 5.168 mm and the two shorter sides approx. 2.5 mm edge length. Two perpendicular longer sides were polished (OP-S using colloidal silica for 15 min, Vibromet for 5 hrs), chemically etched and cleaned to remove surface contamination. The sample was compressed along the longitudinal axis in the testing machine MTS 809 using the displacement  $0.1 \mu\text{m/s}$  to the final length 4.941 mm; the total loading time was 51:40 min. This resulted in 4.4% plastic strain and the engineering strain rate of  $1.4 \times 10^{-5} \text{ s}^{-1}$ . The sample was cleaned in acetone before the following steps.

The two polished surfaces were examined using the Nomarski contrast in an optical microscope, which is extremely sensitive to the variation of the surface relief. One surface of the sample was found to contain very fine slip traces, while these traces were almost invisible on the perpendicular polished surface due to a large density of etch markings. Interestingly, no slip traces were visible in SEM on any surface, which is consistent with the work of Argon and Maloof [2], where slip traces were observed under electron microscope only after 8% of plastic strain!

In Fig. 7 we show a comparison of slip traces on the side A of the sample obtained by Nomarski contrast in an optical microscope with theoretical predictions. The lines in Fig. 7a correspond to the traces of four  $\{110\}\langle 111\rangle$  systems that are predicted to be most operative by the Schmid law. The thickness of each line is proportional to the visibility  $\mathbf{g} \cdot \mathbf{b}$ , where  $\mathbf{g}$  is the viewing direction and  $\mathbf{b}$  the Burgers vector of the dislocation (i.e. the thicker the line the more visible the slip trace should be). According to the Schmid law, the directions of slip traces should correspond to the green and/or cyan thick lines, which is in clear disagreement with the optical micrograph in the background. In Fig. 7b, we carry out a similar analysis but now the slip traces are predicted using the effective yield criterion developed in Refs. [28, 29]. The thick lines colored blue and magenta have the same orientation and correspond to the slip systems with the largest values of  $\tau^*$  and, at the same time, the largest visibility among all slip systems. Their directions are in excellent agreement with the orientation of one family of slip traces obtained by optical microscopy. At the time, it seems that the second family of slip traces is not produced by a single slip but rather it is a product of cross-slip of the dislocation between two  $\{110\}\langle 111\rangle$  systems.



## 4.2 Experiments on free-standing pillars

Very different experiments to understand the origin of plasticity in BCC metals are now under way in the group of Helena van Swygenhoven (Paul Scherrer Institute). These are based on Laue diffraction measurements on in situ compressed micropillars of W. The experiments on micropillars probe the plasticity in volumes that are nearly free of dislocations, which deform by nucleation of new dislocations and their immediate movement toward the surface of the sample. This is quite different from macroscopic samples, where the dislocation has to overcome not only the intrinsic lattice friction (the Peierls barriers) but also complicated interactions with the network of other dislocations.

These pillars have been prepared by focused ion beam (FIB) whose high-energy gallium ions are known to amorphize about 5-10 nm surface layer of the pillar. The results of these measurements have been used to test our theoretical predictions of the activity of the 24 slip systems (see also Fig. 3). In particular, Marichal et al. [53] show that for some loading directions, our yield criterion predicts the correct order of slip activity, while this is worse for orientations, where the slip takes place also on the low-stressed system. As mentioned above, the contribution of this latter system to the total plastic strain is very small and, despite the claims in Refs. [53] and [52], it is not clear whether this constitutes the anomalous slip as defined by Duesbery [14] and Bolton and Taylor [7]. Nevertheless, these experiments may play important role in the parametrization of our yield criterion (4) for materials with strong effects of shear stresses perpendicular to the slip direction (such as W but not Mo). The reason is that the slip activity predicted by the yield criterion depends strongly upon the parameter  $a_2$  in (4) whose precise value cannot be obtained solely from atomistic simulations.

Since the typical distance between dislocations is in the micron range, the surface effects in micron-sized pillars should be so strong that the pillar would be effectively dislocation-free. Hence, the yield stress should equal the stress needed to nucleate a new dislocation loop, which is approximately 1/30th of the theoretical strength. However, Bei et al. [6] showed that these FIB-prepared pillars yielded at much smaller stresses than expected for dislocation-free samples. To understand this difference, they obtained a directionally solidified NiAl-Mo eutectic and etched away the NiAl matrix. This way, they obtained a series of free-standing Mo pillars without any surface damage that were further compressed along their longitudinal axes. Interestingly, these pillars yielded at stresses close to 1/30th of the theoretical strength, which is three to four times higher than the yield stress of the pillars prepared by FIB. This suggests that the surface damage caused by FIB may strongly influence the plasticity of micron-sized pillars.



## REFERENCES

- [1] G. J. Ackland and R. Thetford. An improved n-body semi-empirical model for body-centred cubic transition metals. *Philos. Mag. A*, 56(1):15–30, 1987.
- [2] A. S. Argon and S. R. Maloof. Plastic deformation of tungsten single crystals at low temperatures. *Acta Metall.*, 14:1449–1462, 1966.
- [3] G. R. Barsch and J. A. Krumhansl. Twin boundaries in ferroelastic media without interface dislocations. *Phys. Rev. Lett.*, 53(11):1069–1072, 1984.
- [4] B. Barvinschi, L. Proville, and D. Rodney. Quantum Peierls stress of straight and kinked dislocations and effect of non-glide stresses. *Model. Simul. Mater. Sci. Eng.*, 22:025006, 2014.
- [5] J. L. Bassani and V. Racherla. From non-planar dislocation cores to non-associated plasticity and strain bursts. *Prog. Mater. Sci.*, 56:852–863, 2011.
- [6] H. Bei, S. Shim, E. P. George, M. K. Miller, E. G. Herbert, and G. M. Pharr. Compressive strengths of molybdenum alloy micro-pillars prepared using a new technique. *Scr. Mater.*, 57:397–400, 2007.
- [7] C. J. Bolton and G. Taylor. Anomalous slip in high-purity niobium single crystals deformed at 77 K in tension. *Philos. Mag.*, 26(6):1359–1376, 1972.
- [8] D. Caillard. On the stress discrepancy at low-temperatures in pure iron. *Acta Mater.*, 62:267–275, 2014.
- [9] M. J. Cawkwell. *Interatomic bonding and plastic deformation in iridium and molybdenum disilicide*. PhD thesis, University of Pennsylvania, 2005.
- [10] M. S. Daw and M. I. Baskes. Embedded-atom method: Derivation and application to impurities, surfaces, and other defects in metals. *Phys. Rev. B*, 29(12):6443–6453, 1984.
- [11] A. F. Devonshire. Theory of barium titanate – Part I. *Philos. Mag.*, 40:1040–1063, 1949.
- [12] L. Dezerald, L. Ventelon, E. Clouet, C. Denoual, D. Rodney, and F. Willaime. Ab initio modeling of the two-dimensional energy landscape of screw dislocations in bcc transition metals. *Phys. Rev. B*, 89:024104, 2014.
- [13] J. E. Dorn and S. Rajnak. Nucleation of kink pairs and the Peierls’ mechanism of plastic deformation. *Trans. AIME*, 230:1052–1064, 1964.
- [14] M. S. Duesbery. The influence of core structure on dislocation mobility. *Philos. Mag.*, 19(159):501–526, 1969.
- [15] M. S. Duesbery. On non-glide stresses and their influence on the screw dislocation core in body-centered cubic metals. I. The Peierls stress. *Proc. R. Soc. Lond. A*, 392(1802):145–173, 1984.
- [16] M. S. Duesbery. On non-glide stresses and their influence on the screw

- dislocation core in body-centered cubic metals. II. The core structure. *Proc. R. Soc. Lond. A*, 392(1802):175–197, 1984.
- [17] M. S. Duesbery and R. A. Foxall. A detailed study of deformation of high-purity niobium single crystals. *Philos. Mag.*, 20(166):719–751, 1969.
- [18] M. S. Duesbery, V. Vitek, and D. K. Bowen. The effect of shear stress on the screw dislocation core structures in body-centered cubic lattices. *Proc. R. Soc. Lond. A*, 332:85–111, 1973.
- [19] K. Edagawa, T. Suzuki, and S. Takeuchi. Motion of a screw dislocation in a two-dimensional Peierls potential. *Phys. Rev. B*, 55(10):6180–6187, 1997.
- [20] J. Friedel, G. Leman, and S. Olszewski. On the nature of magnetic couplings in transitional metals. *J. Appl. Phys.*, 32(3):325S–330S, 1961.
- [21] R. G. Garlick and H. B. Probst. Investigation of room-temperature slip in zone-melted tungsten single crystals. *Trans. Metall. Soc. AIME*, 230:1120–1125, 1964.
- [22] T. L. Gilbert. A Lagrangian formulation of the gyromagnetic equation of the magnetic field. *Phys. Rev.*, 100:1243–1243, 1955.
- [23] V. L. Ginzburg and L. D. Landau. On the theory of superconductivity. *Zh. Eksp. Teor. Fiz.*, 20(12):1064–1082, 1950.
- [24] A. Girshick. *Atomistic studies of dislocations in titanium and titanium-aluminum compound*. PhD thesis, University of Pennsylvania, 1997.
- [25] N. Goldenfeld, B. P. Athreya, and J. A. Dantzig. Renormalization group approach to multiscale modelling in materials science. *J. Stat. Phys.*, 125(5/6):1019–1027, 2006.
- [26] R. Gröger. *Development of physically based plastic flow rules for body-centered cubic metals with temperature and strain rate dependencies*. PhD thesis, University of Pennsylvania, 2007.
- [27] R. Gröger. Which stresses affect the glide of screw dislocations in bcc metals? *Philos. Mag.*, 94(18):2021–2030, 2014.
- [28] R. Gröger, A. G. Bailey, and V. Vitek. Multiscale modeling of plastic deformation of molybdenum and tungsten: I. Atomistic studies of the core structure and glide of  $1/2\langle 111 \rangle$  screw dislocations at 0 K. *Acta Mater.*, 56:5401–5411, 2008.
- [29] R. Gröger, V. Racherla, J. L. Bassani, and V. Vitek. Multiscale modeling of plastic deformation of molybdenum and tungsten: II. Yield criterion for single crystals based on atomistic studies of glide of  $1/2\langle 111 \rangle$  screw dislocations. *Acta Mater.*, 56:5412–5425, 2008.
- [30] R. Gröger and V. Vitek. Explanation of the discrepancy between the theoretical and measured yield stresses in body-centered cubic metals. *Philos. Mag. Lett.*, 87(2):113–120, 2007.
- [31] R. Gröger and V. Vitek. Multiscale modeling of plastic deformation of

- molybdenum and tungsten: III. Effects of temperature and plastic strain rate. *Acta Mater.*, 56:5426–5439, 2008.
- [32] R. Gröger and V. Vitek. Constrained Nudged Elastic Band calculation of the Peierls barrier with atomic relaxations. *Model. Simul. Mater. Sci. Eng.*, 20:035019, 2012.
- [33] R. Gröger and V. Vitek. Stress dependence of the Peierls barrier of  $1/2\langle 111 \rangle$  screw dislocations in BCC metals. *Acta Mater.*, 61:6362–6371, 2013.
- [34] R. Gröger and V. Vitek. Determination of positions and curved transition pathways of screw dislocations in bcc crystals from atomic displacements. *Mat. Sci. Eng. A*, 643:203–210, 2015.
- [35] F. Guiu. Slip asymmetry in molybdenum single crystals deformed in direct shear. *Scripta Metall.*, 3:449–454, 1969.
- [36] G. Henkelman and H. Jónsson. Improved tangent estimate in the nudged elastic band method for finding minimum energy paths and saddle points. *J. Chem. Phys.*, 113(22):9978–9985, 2000.
- [37] G. Henkelman, B. P. Uberuaga, and H. Jónsson. A climbing image nudged elastic band method for finding saddle points and minimum energy paths. *J. Chem. Phys.*, 113(22):9901–9904, 2000.
- [38] R. Hill. *The mathematical theory of plasticity*. Clarendon Press, 1998.
- [39] L. Hollang, D. Brunner, and A. Seeger. Work hardening and flow stress of ultrapure molybdenum single crystals. *Mat. Sci. Eng. A*, 319-321:233–236, 2001.
- [40] A. P. Horsfield, A. M. Bratkovsky, M. Fearn, D. G. Pettifor, and M. Aoki. Bond-order potentials: Theory and implementation. *Phys. Rev. B*, 53(19):12694–12712, 1996.
- [41] L. Hsiung. On the mechanism of anomalous slip in bcc metals. *Mat. Sci. Eng. A*, 528:329–337, 2010.
- [42] K. Ito and V. Vitek. Atomistic study of non-Schmid effects in the plastic yielding of bcc metals. *Philos. Mag. A*, 81(5):1387–1407, 2001.
- [43] H. Jónsson, G. Mills, and K. W. Jacobsen. *Classical and Quantum Dynamics in Condensed Phase Simulations*, chapter 16. Nudged elastic band method for finding minimum energy paths of transitions, pages 385–404. World Scientific, Singapore, 1998.
- [44] S. Kartha, J. A. Krumhansl, J. P. Sethna, and L. K. Wickham. Disorder-driver pretransitional tweed pattern in martensitic transformations. *Phys. Rev. B*, 52(2):803–822, 1995.
- [45] L. Kaun, A. Luft, J. Richter, and D. Schulze. Slip line pattern and active slip systems of tungsten and molybdenum single crystals weakly deformed in tension at room temperature. *Phys. Stat. Sol.*, 26(2):485–499, 1968.
- [46] A. Koester, A. Ma, and A. Hartmaier. Atomistically informed crystal

- plasticity model for body-centered cubic iron. *Acta Mater.*, 60:3894–3901, 2012.
- [47] L. P. Kubin. *Dislocations, mesoscale simulations and plastic flow*. Oxford Publications, 2013.
- [48] J. S. Langer. Instabilities and pattern formation in crystal growth. *Rev. Mod. Phys.*, 52(1):1–28, 1980.
- [49] H. Lim, C. R. Weinberger, C. C. Battaile, and T. E. Buchheit. Application of generalized non-Schmid yield law to low temperature plasticity in BCC transition metals. *Model. Simul. Mater. Sci. Eng.*, 21:045015, 2013.
- [50] Y.-S. Lin, M. Mrovec, and V. Vitek. A new method for development of bond-order potentials for transition bcc metals. *Model. Simul. Mater. Sci. Eng.*, 22:034002, 2014.
- [51] F. Louchet, L. P. Kubin, and D. Vesely. In situ deformation of b.c.c. crystals at low temperatures in a high-voltage electron microscope. Dislocation mechanisms and strain-rate equation. *Philos. Mag. A*, 39(4):433–454, 1979.
- [52] C. Marichal, K. Srivastava, D. Weygand, S. Van Petegem, D. Grolimund, P. Gumbsch, and H. Van Swygenhoven. Origin of anomalous slip in tungsten. *Phys. Rev. Lett.*, 113:025501, 2014.
- [53] C. Marichal, H. Van Swygenhoven, S. Van Petegem, and C. Borca.  $\{110\}$  slip with  $\{112\}$  slip traces in bcc tungsten. *Sci. Rep.*, 3:2547, 2013.
- [54] M. Mrovec. *Bond order potentials for bcc transition metals and molybdenum silicides*. PhD thesis, University of Pennsylvania, 2002.
- [55] M. Mrovec, R. Gröger, A. G. Bailey, D. Nguyen-Manh, C. Elsässer, and V. Vitek. Bond-order potential for simulations of extended defects in tungsten. *Phys. Rev. B*, 75:104119, 2007.
- [56] M. Mrovec, D. Nguyen-Manh, D. G. Pettifor, and V. Vitek. Bond-order potential for molybdenum: Application to dislocation behavior. *Phys. Rev. B*, 69:094115, 2004.
- [57] F. R. N. Nabarro. Dislocations in a simple cubic lattice. *Proc. Phys. Soc.*, 59(2):256–272, 1947.
- [58] R. Peierls. The size of a dislocation. *Proc. Phys. Soc.*, 52(1):34–37, 1940.
- [59] D. G. Pettifor. New many body potential for the bond order. *Phys. Rev. Lett.*, 63(22):2480–2483, 1989.
- [60] N. Provatas and K. Elder. *Phase-field methods in material science and engineering*. J. Wiley & Sons, 2010.
- [61] L. Proville, D. Rodney, and M.-C. Marinica. Quantum effect on thermally activated glide of dislocations. *Nature Mater.*, 11:845, 2012.
- [62] L. Proville, L. Ventelon, and D. Rodney. Prediction of the kink-pair formation enthalpy on screw dislocations in  $\alpha$ -iron by a line tension model parametrized on empirical potentials and first-principles calcula-

- tions. *Phys. Rev. B*, 87:144106, 2013.
- [63] Q. Qin and J. L. Bassani. Non-associated plastic flow in single crystals. *J. Mech. Phys. Sol.*, 40(4):835–862, 1992.
- [64] Q. Qin and J. L. Bassani. Non-Schmid yield behavior in single crystals. *J. Mech. Phys. Sol.*, 40(4):813–833, 1992.
- [65] D. Rodney and L. Proville. Stress-dependent Peierls potential: Influence on kink-pair activation. *Phys. Rev. B*, 79:094108, 2009.
- [66] R. M. Rose, D. P. Ferriss, and J. Wulff. Yielding and plastic flow in single crystals of tungsten. *Trans. Metall. Soc. AIME*, 224:981–990, 1962.
- [67] E. Schmid and W. Boas. *Plasticity of crystals with special reference to metals*. F. A. Hughes & Co., 1950.
- [68] K. Srivastava, R. Gröger, D. Weygand, and P. Gumbsch. Dislocation motion in tungsten: Atomistic input to discrete dislocation simulations. *Int. J. Plast.*, 47:126–142, 2013.
- [69] E. H. Stanley. *Introduction to phase transitions and critical phenomena*. Oxford Science Publications, 1987.
- [70] T. Suzuki, H. Koizumi, and H. O. K. Kirchner. Plastic flow stress of b.c.c. transition metals and the Peierls potential. *Acta Metall. Mater.*, 43(6):2177–2187, 1995.
- [71] G. I. Taylor. The deformation of crystals of  $\beta$ -brass. *Proc. R. Soc. Lond. A*, 118(779):1–24, 1928.
- [72] G. I. Taylor and C. F. Elam. The distortion of iron crystals. *Proc. Roy. Soc. Lond. A*, 112(761):337–361, 1926.
- [73] G. Tsekenis, J. T. Uhl, N. Goldenfeld, and K. A. Dahmen. Determination of the universality class of crystal plasticity. *Europhys. Lett.*, 101:36003, 2013.
- [74] L. Ventelon, F. Willaime, E. Clouet, and D. Rodney. Ab initio investigation of the Peierls potential of screw dislocations in bcc Fe and W. *Acta Mater.*, 61(11):3973–3985, 2013.
- [75] V. Vitek, M. Mrovec, R. Gröger, J. L. Bassani, V. Racherla, and L. Yin. Effects of non-glide stresses on the plastic flow of single and polycrystals of molybdenum. *Mat. Sci. Eng. A*, 387-389:138–142, 2004.
- [76] C. R. Weinberger, C. C. Bataille, T. E. Buchheit, and Holm. E. A. Incorporating atomistic data of lattice friction into BCC crystal plasticity models. *Int. J. Plast.*, 37:16–30, 2012.
- [77] K. G. Wilson. Problems in physics with many scales of length. *Sci. Amer.*, 1979.
- [78] S. Znam. *Bond-order potentials for atomistic studies of dislocations and other extended defects in TiAl*. PhD thesis, University of Pennsylvania, 2001.

## SELECTED IMPACT PUBLICATIONS

- Fikar J., **Gröger R.**: Interactions of prismatic dislocation loops with free surfaces in thin foils of body-centered cubic iron. *Acta Mater.* 99:392-401 (2015).
- Gröger R.**, Vitek V.: Determination of positions and curved transition pathways of screw dislocations in BCC crystals from atomic displacements. *Mat. Sci. Eng. A* 643:203-210 (2015).
- Gröger R.**, Leconte L., Ostapovets, A.: Structure and stability of threading edge and screw dislocations in bulk GaN. *Comp. Mater. Sci.* 99:195–202 (2015).
- Gröger R.**: Which stresses affect the glide of screw dislocations in bcc metals? *Philos. Mag.* 94(18):2021–2030 (2014).
- Ostapovets A., **Gröger R.**: Twinning disconnections and basal-prismatic twin boundary in magnesium. *Model. Simul. Mater. Sci. Eng.* 22:025015 (2014).
- Gröger R.** and Vitek, V.: Stress dependence of the Peierls barrier of  $1/2\langle 111 \rangle$  screw dislocations in BCC metals. *Acta Mater.* 61:6362–6371 (2013).
- Srivastava K., **Gröger R.**, Weygand D., Gumbsch P.: Dislocation motion in tungsten: Atomistic input to discrete dislocation simulations. *Int. J. Plast.* 47:126–142 (2013).
- Gröger R.** and Vitek V.: Constrained Nudged Elastic Band calculation of the Peierls barrier with atomic relaxations. *Model. Simul. Mater. Sci. Eng.* 20:035019 (2012).
- Gröger R.**, Dudeck K. J., Nellist P. D., Vitek V., Hirsch P. B., Cockayne D. J. H.: Effect of Eshelby twist on core structure of screw dislocations in molybdenum: Atomic structure and electron microscope image simulations. *Philos. Mag.* 91(18):2364–2381 (2011).
- Gröger R.**, Lookman T., Saxena A.: Incompatibility of strains and its application to mesoscopic studies of plasticity. *Phys. Rev. B* 82(14):144104 (2010).
- Gröger R.**, Vitek, V.: Temperature and strain rate dependent flow criterion for bcc transition metals based on atomistic analysis of dislocation glide. *Int. J. Mater. Res.* 100(3):315–321 (2009).
- Gröger R.** and Vitek V.: Directional versus central-force bonding in studies of the structure and glide of  $1/2\langle 111 \rangle$  screw dislocations in bcc transition metals. *Philos. Mag.* 89(34):3163–3178 (2009).
- Gröger R.**, Lookman T., Saxena, A.: Atomistic studies of transformation pathways and energetics in plutonium. *Philos. Mag.* 89:1779–1792 (2009).

- Gröger R.**, Vitek V.: Multiscale modeling of plastic deformation of molybdenum and tungsten: III. Effects of temperature and plastic strain rate. *Acta Mater.* 56:5426–5439 (2008).
- Gröger R.**, Racherla V., Bassani J. L., Vitek V.: Multiscale modeling of plastic deformation of molybdenum and tungsten: II. Yield criterion for single crystals based on atomistic studies of glide of  $1/2\langle 111 \rangle$  screw dislocations. *Acta Mater.* 56:5412–5425 (2008).
- Gröger R.**, Bailey A. G., Vitek V.: Multiscale modeling of plastic deformation of molybdenum and tungsten: I. Atomistic studies of the core structure and glide of  $1/2\langle 111 \rangle$  screw dislocations at 0 K. *Acta Mater.* 56:5401–5411 (2008).
- Gröger R.**, Vitek V.: Explanation of the discrepancy between the theoretical and measured yield stresses in body-centered cubic metals. *Philos. Mag. Lett.* 87(2):113–120 (2007).
- Mrovec M., **Gröger R.**, Bailey A. G., Nguyen-Manh D., Elsässer C., Vitek V.: Bond-order potential for simulations of extended defects in tungsten. *Phys. Rev. B* 75:104119 (2007).
- Nguyen-Manh D., Cawkwell M. J., **Gröger R.**, Mrovec M., Porizek R., Pettifor D. G., Vitek V.: Dislocations in materials with mixed covalent and metallic bonding. *Mat. Sci. Eng. A* 400-401:68–71 (2005).
- Vitek V., Mrovec M., **Gröger R.**, Bassani J. L., Racherla V., Yin L.: Effects of non-glide stresses on the plastic flow of single and polycrystals of molybdenum. *Mat. Sci. Eng. A* 387-389:138–142 (2004).

## ABSTRACT

The plastic deformation of body-centered cubic (BCC) metals is not governed by the same processes as in close-packed crystal structures. Over the past 12 years, we have developed a new description of plasticity in BCC metals that is based on detailed understanding of the atomic-level processes affecting the glide of  $1/2\langle 111 \rangle$  screw dislocations at 0 K. These have been incorporated into thermodynamic models of dislocation glide at finite temperatures and strain rates. To complement these theoretical efforts, we have recently initiated a systematic experimental program whose objective is to provide direct experimental evidence of the activity of individual  $\{110\}\langle 111 \rangle$  slip systems, conditions under which dislocations cross-slip between different systems, and to assess the predictive capability of our theoretical models. Combining these theoretical, computational and experimental results is expected to shed light onto many puzzling phenomena such as the origin of the anomalous slip and thus ultimately close the gap in understanding plasticity of all BCC metals.